

# Inhibition of Musashi-1 enhances chemotherapeutic sensitivity in gastric cancer patient-derived xenografts

Fan Liu<sup>1,2,3</sup>, Huan Yang<sup>2</sup>, Xinyu Zhang<sup>2</sup>, Xianglin Sun<sup>2</sup>, Jiamin Zhou<sup>2</sup>, Yuan Li<sup>4</sup>, Yifei Liu<sup>4</sup>, Zhixiang Zhuang<sup>1</sup> and Guohua Wang<sup>2</sup> 

<sup>1</sup>Department of Oncology, The Second Affiliated Hospital of Soochow University, Suzhou 215004, China; <sup>2</sup>Department of Physiology and Hypoxic Biomedicine, Institute of Special Environmental Medicine, Nantong University, Nantong 226019, China; <sup>3</sup>Department of Oncology, Affiliated Hospital of Nantong University, Nantong 226001, China; <sup>4</sup>Department of Pathology, Affiliated Hospital of Nantong University, Nantong 226001, China

Corresponding authors: Guohua Wang. Email: wgh036@hotmail.com; Zhixiang Zhuang. Email: 13951106391@139.com

## Impact Statement

MSI1, a member of the Musashi (MSI) family, is normally expressed in epithelial progenitor cells in the gastric mucosa. Here, we investigated the relationship between MSI1 expression and the efficacy of chemical drugs in gastric cancer. Using MSI1 overexpression and silencing in cell systems, we found that MSI1 expression is strongly associated with cell proliferation, migration, and invasion, and plays a significant role in the occurrence and progression of gastric cancer. Experiments in patient-derived xenograft mouse models showed that MSI1 inhibition increased the efficacy of chemical drugs used for treating gastric cancer. MSI1 influenced the therapeutic effects of chemotherapy mainly through blood vessel epicardial substance (BVES) molecular pathways. This study may provide insight into the application of personalized therapy for gastric cancer, and may be of value in predicting the chemosensitivity of cancer and the development of more effective gene-directed prodrug therapy.

## Abstract

Musashi-1 (MSI1), a neural RNA-binding protein, is considered a gastric and intestinal stem cell marker. Although the function of MSI1 in gastric cancer has attracted increasing interest, it is not known whether MSI1 can be used as a biomarker to monitor gastric cancer development and response to treatment. Here, the role of MSI1 in the chemotherapeutic sensitivity of gastric cancer was investigated. Patients with high MSI1 levels had poor outcomes, implicating the gene in the development and progression of the disease. We overexpressed and silenced MSI1 in the human gastric cancer cell lines MKN45 and HGC27, finding that knockdown reduced proliferation, invasion, and migration, while promoting apoptosis. A patient-derived xenograft gastric cancer model was constructed in which mice received chemical drugs, si-MSI1, or a drug-si-MSI1 combination. It was found that blocking MSI1 expression reduced gastric cancer drug tolerance. The combination treatment with si-MSI1 was superior to 5F-dUMP and cisplatin, either separately or in combination, indicating that including si-MSI1 was better than drug therapy alone. Transcriptome sequencing analysis showed that MSI1 altered cell cycle regulation and growth signal transduction, including that of blood vessel epicardial substance (BVES). These results suggest that MSI1 reduces the tolerance of gastric cancer to chemical drugs through modulation of MSI1/BVES signaling.

**Keywords:** Musashi-1, chemotherapy sensitivity, patient-derived xenograft, gastric cancer, RNA sequencing

**Experimental Biology and Medicine 2022; 247: 868–879. DOI: 10.1177/15353702221076793**

## Introduction

Gastric cancer is a common digestive malignancy and ranks second in responsibility for cancer-related deaths.<sup>1</sup> Metastatic disease is usually treated by chemotherapy, but its effect is limited,<sup>2</sup> and patient survival is generally poor, with a median of 8–11 months.<sup>3</sup> Apart from distant metastases, drug resistance accounts for much of the morbidity and mortality of gastric cancer, and this has become a worldwide problem.<sup>4</sup> Gene-targeted therapy has already shown significant promise for preventing gastric cancer progression, suggesting the

value of searching for more effective gene-directed prodrug therapies for gastric cancer.<sup>5–7</sup>

The *musashi* (*msi*) gene was initially identified in *Drosophila* and encodes an RNA-binding protein.<sup>6,8</sup> Humans have two homologs of the gene, Musashi-1 (MSI1) and Musashi-2 (MSI2).<sup>9</sup> MSI1 is expressed at high levels in neural stem cells and was initially identified as a neural stem cell marker.<sup>10</sup> Recently, MSI1 has been discovered in tissues outside the nervous system and has been recognized as a potential marker of gastric and intestinal stem cells.<sup>11</sup> High expression levels of MSI1 in astrocytoma and glioma are indicative

of poor prognosis.<sup>9</sup> MSI1 has been found to be upregulated in renal carcinoma, where it appears to be closely involved in both invasion and metastasis.<sup>12</sup>

MSI1 expression in gastric cancer-derived cell lines also appears to be high.<sup>13</sup> It has been found that an early event in gastric carcinogenesis is MSI1-positive cell expansion. MSI1-positive cells show different levels of proliferation between gastric cancer and precancerous lesions.<sup>11</sup> Moreover, MSI1 was found to be markedly upregulated in the tissues of gastric cancer patients and was closely associated with the progression and poor prognosis of the disease, as shown by a comparison between the analysis of endoscopic biopsy antral specimens and clinicopathological parameters.<sup>14,15</sup> Thus, the function of MSI1 in gastric cancer has attracted increasing interest.<sup>16</sup>

Gastric cancer recurrence has been attributed to the acquisition of resistance to therapeutic drugs and stemness by the neoplastic cells.<sup>17</sup> MSI1 may represent a cancer biomarker and may also be a therapeutic target in counteracting drug resistance. However, the basic research into the role of MSI1 in gastric cancer is limited, and the question of the effectiveness of MSI1 in monitoring gastric cancer development and response to treatment remains unanswered. Investigation is needed to determine the part played by MSI1 in gastric cancer, both *in vitro* and in xenograft studies.

Here, samples from 115 patients with early-stage gastric cancer were collected. We used immunohistochemistry (IHC) to show that MSI1 expression in tumor samples was significantly greater than in the adjacent normal tissue, and that MSI1 levels corresponded with both patient outcomes and the expression of important indicators of cell division, such as proliferating cell nuclear antigen (PCNA) and Ki-67. Therefore, we considered whether the MSI1 protein could be used as a prognostic indicator and a therapeutic target for gastric cancer. We further established a patient-derived xenograft (PDX) model that maintained the basic characteristics of the patient's tumor tissue, including the tumor histopathology and microenvironment.<sup>18,19</sup> We also investigated the relationship between MSI1 tumor expression and the efficacy of clinical chemotherapy drugs to guide the individualized treatment of gastric cancer patients. Moreover, through interfering with MSI1 expression in PDX models, we investigated whether MSI1 is a key modulator of tumor progression and response to therapy and investigated the potential molecular pathways by transcriptome analysis.

## Materials and methods

### Tissue specimens

Data from 115 patients with gastric cancer who had received no preoperative treatment were obtained from the archives of the Department of Pathology, Affiliated Hospital of Nantong University. The fresh samples had been fixed in 4% paraformaldehyde for 24 h, paraffin-embedded, and sectioned for IHC. The control samples were from normal gastric mucosal epithelia. All human tissue collection procedures were approved by the Ethics Committee of the Affiliated Hospital of Nantong University. Written informed consent from all patients was acquired before the study.

### IHC

IHC was conducted as previously described.<sup>20</sup> The antibodies used were anti-MSI1 (Abcam, ab21628), anti-Ki-67 (Abcam, 15580), and anti-PCNA (Abcam, ab18197) polyclonal antibodies (diluted 1:500). MSI1-positive results were defined as cells containing evenly stained yellow or brown cytoplasmic granules. A scoring system combining the proportion of immunoreactive cells with the intensity of immunostaining was used to evaluate immunoreactivity, as previously described.<sup>11,15</sup> Specifically, the staining intensity was scored as 0 (less than 1% positive cells), 1 (1–25% positive cells), 2 (26–50% positive cells), 3 (51–75% positive cells), and 4 (more than 75% positive cells).

### Cell lines and cell culture

All cells were purchased from CBY Life Science & Technology (short tandem repeat (STR) identification provided; Nanjing, China). The human gastric cancer lines SGC-7901, MGC803, MKN45, and HGC27 were maintained in RPMI 1640 medium (Gibco BRL, Grand Island, NY, USA) supplemented with 10% fetal bovine serum (FBS, Gibco). The normal gastric epithelial line GES-1 was grown in keratinocyte serum-free medium (Invitrogen, Carlsbad, CA, USA). All cells were incubated at 37 °C with 5% CO<sub>2</sub>.

### MSI1 transfection

The MSI1-overexpression plasmid (pcDNA3.1-MSI1) and its control vector plasmid were designed for this study and verified by sequencing. Short-hairpin MSI1 siRNA synthesized by Sangon Biotech Co., Ltd. (Shanghai, China) was inserted into pSUPER by enzymatic digestion, and the plasmid was constructed by transfection, followed by selecting and extracting the plasmid. The target sequences used for the siRNA sequences were (shown in sense/antisense pairs): MSI1 siRNA1, 5'-ACAAAGAUCUUCUUCGUUCGA-3' and 5'-GAACGAAGAAGAUCUUCUUCGUGG-3'; MSI1 siRNA2, 5'-AUGAAUUUCACACACUUUCUC-3' and 5'-GAAAGUGUGUGAAAUUCAUUU-3'; MSI1 siRNA3, 5'-UGUUGAUUUC AUGAAAUGAA-3' and 5'-CAUUUU CAUGAAAUCAACAAC-3'. MKN45 and HGC27 cells were transfected to induce overexpression or knockdown using Lipofectamine 2000 (Thermo Fisher Scientific, USA) following the supplied directions, and incubated at 37 °C for 48 h.

### RNA extraction and quantitative real-time polymerase chain reaction analysis

Total RNA was isolated from MKN45 and HGC27 cells using TRIzol reagent (Invitrogen, Carlsbad, CA, USA) according to the manufacturer's protocol. Two picograms of RNA were used to reverse-transcribe cDNA using a cDNA synthesis kit (Tiangen Biotech, China), and the rest was frozen at –80 °C. Real-time polymerase chain reaction analysis (RT-PCR) was performed using a Corbett Research Rotor-Gene 3000 Real-time Thermal Cycler (Corbett Research, Cambridge, UK) and SYBR Green Detection Kit (Invitrogen, Waltham, MA, USA). Relative expression levels were determined by the 2<sup>-ΔΔCT</sup> method, SPSS 17.0 (SPSS, Chicago, IL, USA) was used for analyzing the data, and the data were mapped using SigmaPlot 10.0. The following sequences were used:

MSI1, sense 5'-GATCCAGGGGTTTCGGCTTC-3' and antisense 5'-GAAGGCCACCTTAGGGTCAA-3';  $\beta$ -actin, sense 5'-GATGAGATTGGCATGGCTTT-3' and antisense 5'-GTCACCTTCACCGTTCCAGT-3'.

### Cell viability assay

MKN45 and HGC27 cell growth was measured by the MTT assay. Briefly, MKN45 and HGC27 cells ( $2 \times 10^3$ /well) were plated in 96-well plates, and 20  $\mu$ L 3-(4,5-dimethylthiazol-2-yl)-2,5-diphenyltetrazolium bromide (MTT; 1  $\mu$ g/mL) solution was added and incubated for 6 h under normal culture conditions. After removal of the liquid, 200  $\mu$ L of DMSO was added for crystal dissolution, and absorbances at 570 nm were recorded in an automatic quantitative microplate reader for four consecutive days.

### Cell apoptosis and cell cycle

MKN45 and HGC27 cells were plated ( $4 \times 10^5$  cells/well) in six-well plates and transfected to silence or overexpress MSI1, as described above. The cells were then harvested, washed, and incubated with Annexin V-FITC/propidium iodide (PI) (Invitrogen, Carlsbad, CA, USA) or PI only. Apoptosis and cell cycle evaluation was undertaken on a FACSCalibur flow cytometer (BD, USA).

### Transwell chamber-Matrigel invasion and migration assays

Cell migration and invasion were detected by Transwell assays, as previously described.<sup>21</sup> MSI1-overexpressing or silenced cells in serum-free medium ( $1 \times 10^5$  cells, respectively) were placed in the upper chamber of a 24-well Transwell plate (8 mm pore size; BD Biosciences, USA). To measure migration, the transfected cells were cultured until 80–90% confluent. The lower chamber contained medium with 600  $\mu$ L DMEM containing 10% FBS. After incubation for 24 h, the non-migrated cells in the upper wells were gently removed from the membrane, while cells on the lower sides of the membranes were fixed (4% paraformaldehyde, 10 min) and stained (0.1% crystal violet, 30 min). The cells were examined under light microscopy (magnification 200 $\times$ ), photographed, and the cells in a minimum of five fields were counted. For the detection of cell invasion, the upper chamber was precoated with Matrigel, and the remaining steps were the same as those of the migration assay.

### Establishment of a PDX model for gastric cancer

Before obtaining gastric cancer specimens, the patients signed an informed consent after obtaining their verbal consent. The use of animals in the experiment followed the principles of animal protection. Nude mice, four to six weeks old, were maintained under pathogen-free conditions and acclimatized for at least three days before treatment. The tumor tissue was surgically excised and kept in RPMI medium containing 20% FBS and 0.05% cyan/streptomycin on ice. After removal of damaged or necrotic tissue, the remainder was sliced into pieces (approximately  $2 \times 2 \times 3$  mm<sup>3</sup>). The mice were anesthetized using isoflurane and the abdominal skin was swabbed with disinfectant. A single axillary

incision of approximately 3–5 mm (larger incisions would result in the tumor sliding out easily) was made, followed by 18 punctures with the needle head for blunt separation, and the tumor tissue was inserted into the designated area, along with a drop of 100 $\times$  green/streptomycin. The remaining tumor tissues were either rapidly frozen in liquid nitrogen or paraffin-embedded. The tumor volumes, calculated from the long and short diameters of the tumor, and the body weights of the mice were measured daily or at intervals appropriate for the growth of the tumor. When tumors approximated 1000–1500 mm<sup>3</sup>, the animals were sacrificed, the tumors were removed, and the bodies of the mice were placed in 75% ethanol for 2 min. The tumors were treated as described above.

### Effect of MSI1 silencing on chemotherapeutic sensitivity

The PDX gastric cancer model of gastric cancer was used at passages 3–7 for efficacy evaluation. When tumors approximated 100–200 mm<sup>3</sup> in size, the animals were randomly assigned to one of seven groups, with five to six animals per group. The concentration of 5-Fluorouracil (5-Fu) and cisplatin (DDP) was determined as previously described<sup>22,23</sup> with some modifications. The groups were treated as follows: group 1, control, received intraperitoneal injections of 50 mg/kg saline for three days with administration of the negative control siRNA lentivirus ( $1.5 \times 10^4$  IFU/mL, 0.5 mL) via intratumoral injection; group 2 received si-MSI1 lentivirus ( $1.5 \times 10^4$  IFU/mL, 0.5 mL) intratumorally; group 3 received 50 mg/kg 5-Fu by gavage per day; group 4 were administered intraperitoneal injections of 5 mg/kg DDP per day; group 5 were given 50 mg/kg of 5-Fu and 5 mg/kg DDP per day; group 6 were given 5 mg/kg DDP daily and si-MSI1 lentivirus ( $1.5 \times 10^4$  IFU/mL, 0.5 mL); group 7 received 50 mg/kg 5-Fu daily and si-MSI1 lentivirus ( $1.5 \times 10^4$  IFU/mL, 0.5 mL). The total treatment time was 15 days. The mice were carefully monitored for adverse effects of MSI1 silencing and tumor sizes, as well as their general well-being, in terms of appetite, behavior, and activity. The relative tumor growth inhibition (TGI) was calculated as "TGI = 1 - T/C," where "T/C" indicates the ratio of the tumor volumes of the treated versus control groups. Tumor sizes were measured every three days and the volumes were calculated as "(long diameter  $\times$  short diameter<sup>2</sup>)/2." When tumors approximated 1000–1500 mm<sup>3</sup>, the animals were killed by anesthetic overdose with subsequent cervical dislocation, and the tumors were harvested for immunohistochemical and other analyses.

### Western blotting

The total protein was isolated from the tumors using a kit from Applygen Technologies Inc. (Beijing, China), and the concentration was measured with a BCA Protein Assay Kit (Beyotime, Beijing, China). Samples were then transferred to PVDF, blocked, and probed with primary antibodies (anti-MSI1: polyclonal antibody, Abcam, ab21628, 1:1,000; anti-BVES: polyclonal antibody, GeneTex, GTX30098, 1:1000) overnight at 4  $^{\circ}$ C. The blots were washed with PBS and probed with an HRP-conjugated secondary antibody (Fermentas, Vilnius, Lithuania; 1:1000) for 1 h at room temperature. The loading control was glyceraldehyde

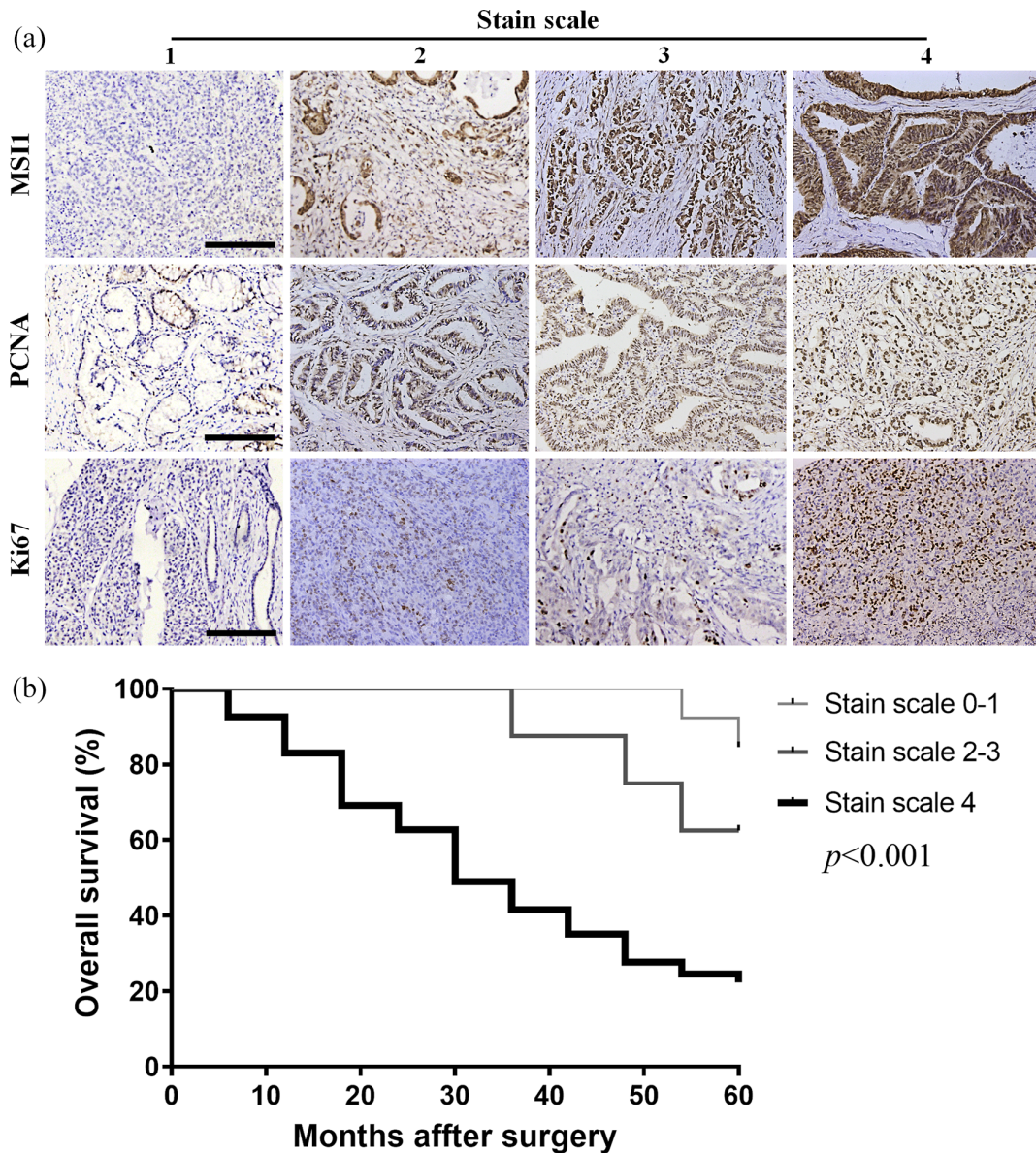


**Figure 1.** Effect of MSI1 expression on gastric cancer progression and survival analysis. (a) Immunohistochemical detection and staining scale of MSI1, Ki-67, and PCNA in gastric cancer tissues. Association between MSI1 expression and clinicopathological markers in patients with gastric cancer. (b) Correlation of survival rate with MSI staining scale score (scale bar = 200  $\mu$ m). (A color version of this figure is available in the online journal.)

3-phosphate dehydrogenase (GAPDH). An Odyssey laser scanning system was used for visualization.

#### RNA-seq analysis

Total RNA was extracted from the various groups, its purity checked on agarose gels, and the concentrations measured spectrophotometrically using RNase-free water as reference. The sequencing of the transcriptome was conducted by Majorbio (Shanghai, China) and differential expression of genes was analyzed using the Majorbio Cloud Platform (www.majorbio.com).

#### Statistical analysis

Data were expressed as mean values and standard deviations. Differences between groups were determined by

one-way analysis of variance (ANOVA) using SPSS 17.0. Relationships between MSI1 expression and clinical and pathological features were determined by the  $\chi^2$  test. All experiments were repeated a minimum of three times. A value of  $P < 0.05$  was defined as statistically significant.

## Results

### Effect of MSI1 expression on gastric cancer progression

IHC analysis of MSI1 expression in patient samples (Figure 1(a)) showed that, despite differences between different patients, overall, there was a strong correlation between MSI1 and the levels of the proliferation markers Ki-67 and PCNA (Figure 1(a) and Table 1, all  $P < 0.01$ ). Moreover, patients with a classification of 4 on the IHC scale had significantly reduced

**Table 1.** Association between MSI1 expression with clinicopathological markers (Ki-67 and MSI1) in patients with gastric cancer.

Marker	Total	Stain scale					$\chi^2$ value	P value
		0	1	2	3	4		
PCNA	108	2	2	15	29	60	38.3353	0.0000
Ki-67	108	3	50	25	24	6	137.9366	0.0000
MSI1	115	5	8	5	3	94	–	–

Each group was compared with the MSI1 group, and statistical analyses were carried out using Pearson's  $\chi^2$  test.  $P < 0.01$  was considered significant.

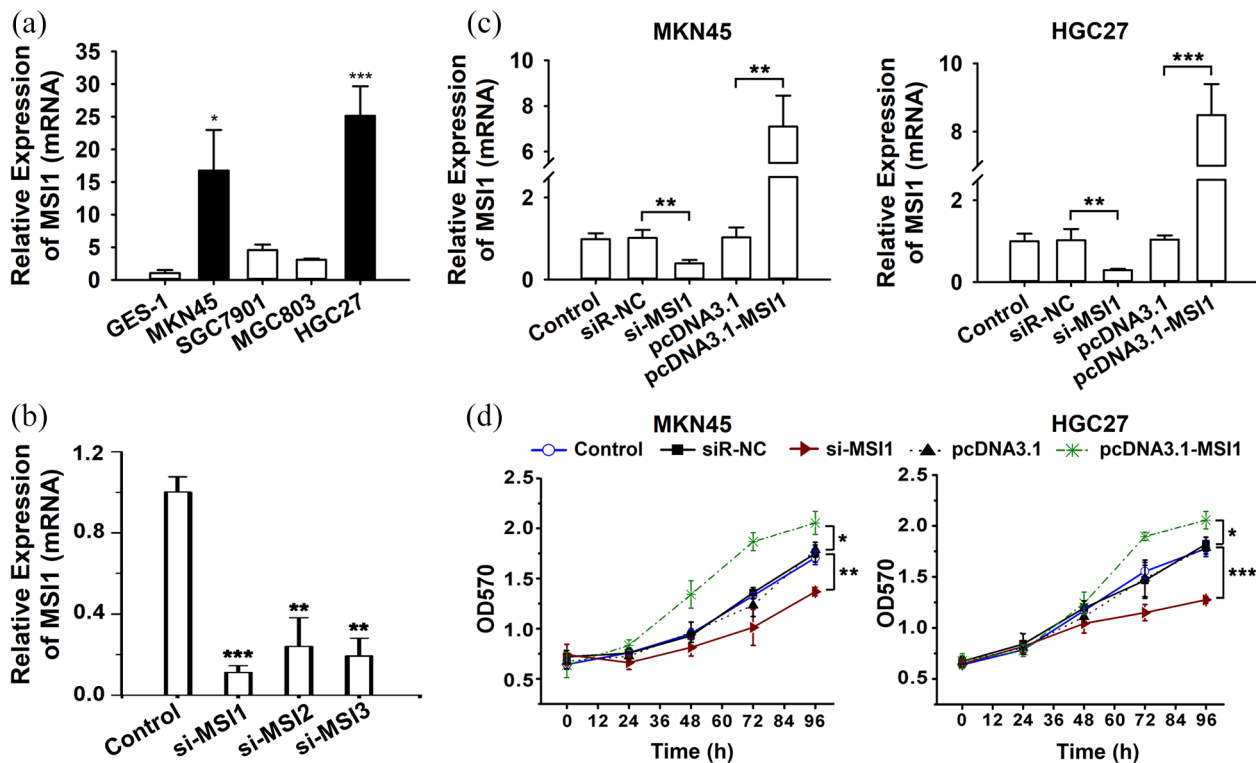


**Figure 2.** Effect of MSI1 interference on gastric cell proliferation ability. (a) qPCR analysis of MSI1 expression in different gastric cancer cell lines and normal gastric mucosa cells ( $*P < 0.05$ ;  $***P < 0.001$  vs GES-1 cells). (b) The optimal knockdown effect was noted with MSI1-siRNA1, which was used in the subsequent experiments. (c) qPCR verified the interference efficiency of MSI1 ( $**P < 0.01$ ;  $***P < 0.001$ ). (d) The effect of MSI1 interference on cell proliferation abilities was determined by MTT assay ( $n = 8-10$  per group;  $*P < 0.05$ ;  $**P < 0.01$ ;  $***P < 0.001$ ). (A color version of this figure is available in the online journal.)

survival compared with those on scales 0–1 and 2–3 (Figure 1(b),  $P > 0.05$ ). This suggests that the importance of MSI1 to the development and progression of gastric cancer.

### Effect of MSI1 gene silencing on proliferation

Both *in vitro* experiments and the transcriptome sequencing data indicated that MSI1 levels were considerably higher in the gastric cancer cell lines (HGC27 and MKN45) than in cells derived from normal mucosa or other types of cancer (Figure 2(a), all  $P < 0.01$ ). All the siRNAs were effective in targeting MSI1, with MSI1-siRNA1 the most effective (Figure 2(b),  $P < 0.001$ ), and this siRNA was used for subsequent experiments. Silencing was found to prevent MSI1 mRNA expression effectively in HGC27 and MKN45 cells, while pcDNA3.1-MSI1 was effective in increasing MSI1 mRNA (Figure 2(c), all  $P < 0.01$ ). Silencing also significantly reduced proliferation in the gastric cancer lines compared to

the control (siRNA-NC vs si-MSI1), while pcDNA3.1-MSI1 promoted proliferation (pcDNA3.1 vs pcDNA3.1-MSI1), as shown by the MTT assay (Figure 2(d),  $P < 0.05$  or  $P < 0.01$ ). These results indicate that silencing of the MSI1 gene blocks gastric cancer cell growth.

### Effect of MSI1 gene silencing on apoptosis and the cell cycle

As seen in Figures 3 and 4, no changes in cell apoptosis or the cell cycle were visible in the siRNA-NC and pcDNA3.1 vector groups. In Figure 3, it is apparent that apoptosis increased after MSI1 knockdown but was also elevated after pcDNA3.1-MSI1 overexpression in both HGC27 and MKN45 cells ( $P < 0.05$  or  $P < 0.01$ ). The apoptosis rate in the si-MSI1 group was higher than for other treatments, indicating that MSI1 silencing induces apoptosis. We examined the DNA cellular contents to analyze the cell cycle distribution

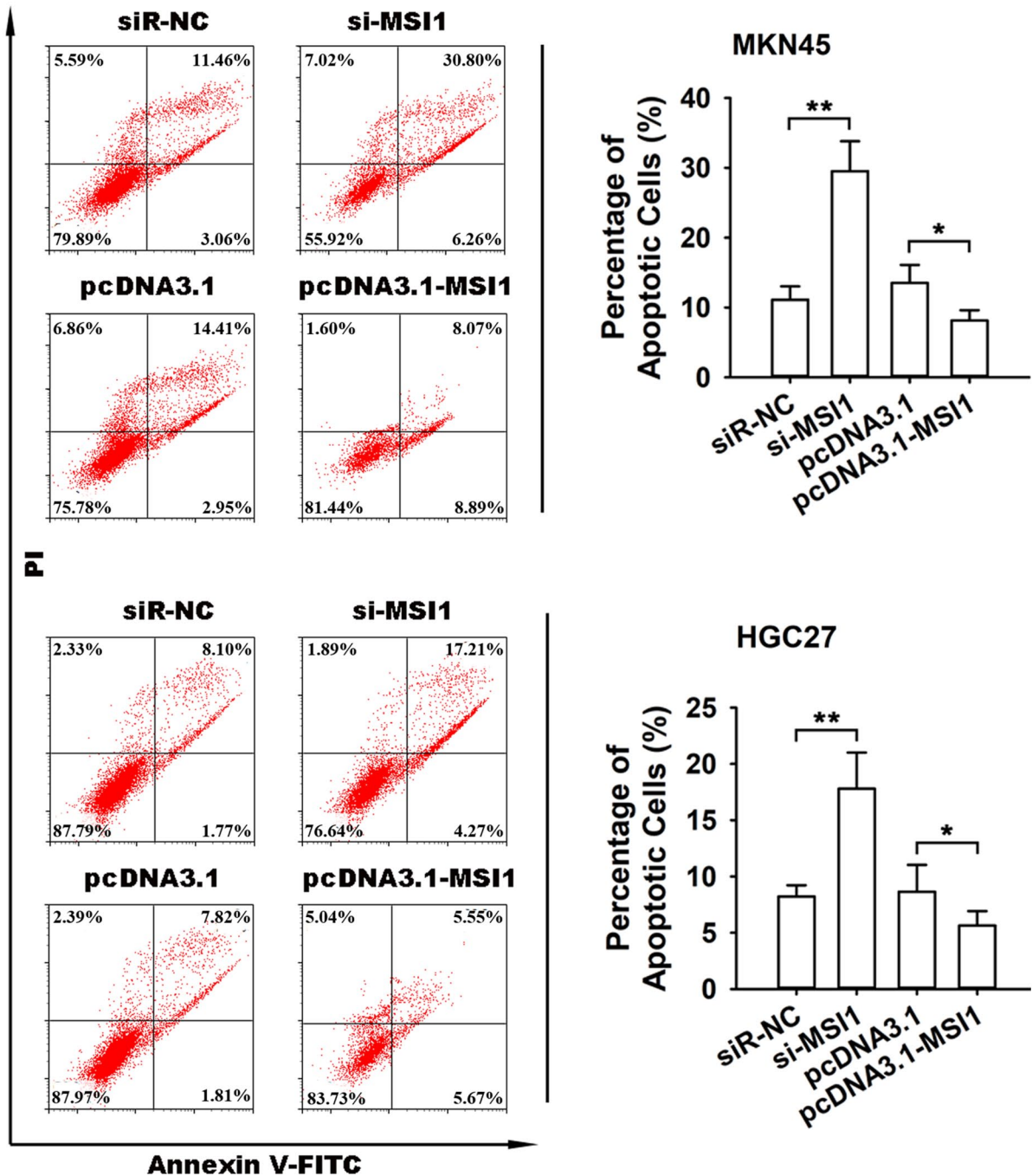


**Figure 3.** Effect of MSI1 interference on cell apoptosis. Apoptosis in MKN45 and HGC27 cells was assessed using the Annexin V-FITC/PI Apoptosis Detection kit, and fluorescence-activated cell sorting analysis was performed. The upper right quadrant (Q2-2; Annexin V+/PI+) indicates apoptosis ( $n=3$ ;  $**P < 0.01$ ). (A color version of this figure is available in the online journal.)

(Figure 4), comparing the distributions of cells over the cell cycle. This showed that, compared with the control, siRNA-MSI1 transfection increased the percentage of MKN45 tumor cells in G2/M phase. Interestingly, the percentage of cells in the G2/M phase was decreased by siRNA-MSI1 transfection in HGC27 cells and was mostly arrested in S phase.

#### Effects of MSI1 gene silencing on cell migration and invasion

Neither siRNA-NC nor pcDNA3.1 affected migration in either of the gastric cancer lines, compared with the control,

while migration (Figure 5(a) and (b),  $P < 0.05$  or  $P < 0.01$ ) and invasion (Figure 5(c) and (d),  $P < 0.05$  or  $P < 0.01$ ) were reduced after si-MSI1 treatment. Both invasion and migration in the pcDNA3.1-MSI1 group were elevated compared to the vector group, indicating that MSI1 overexpression stimulated these processes significantly in gastric cancer cells (Figure 5).

#### MSI1 gene silencing inhibited tumor growth in the PDX mouse model *in vivo*

To further investigate the part played by MSI1 in gastric cancer, we established gastric PDX mouse models. Lentiviral

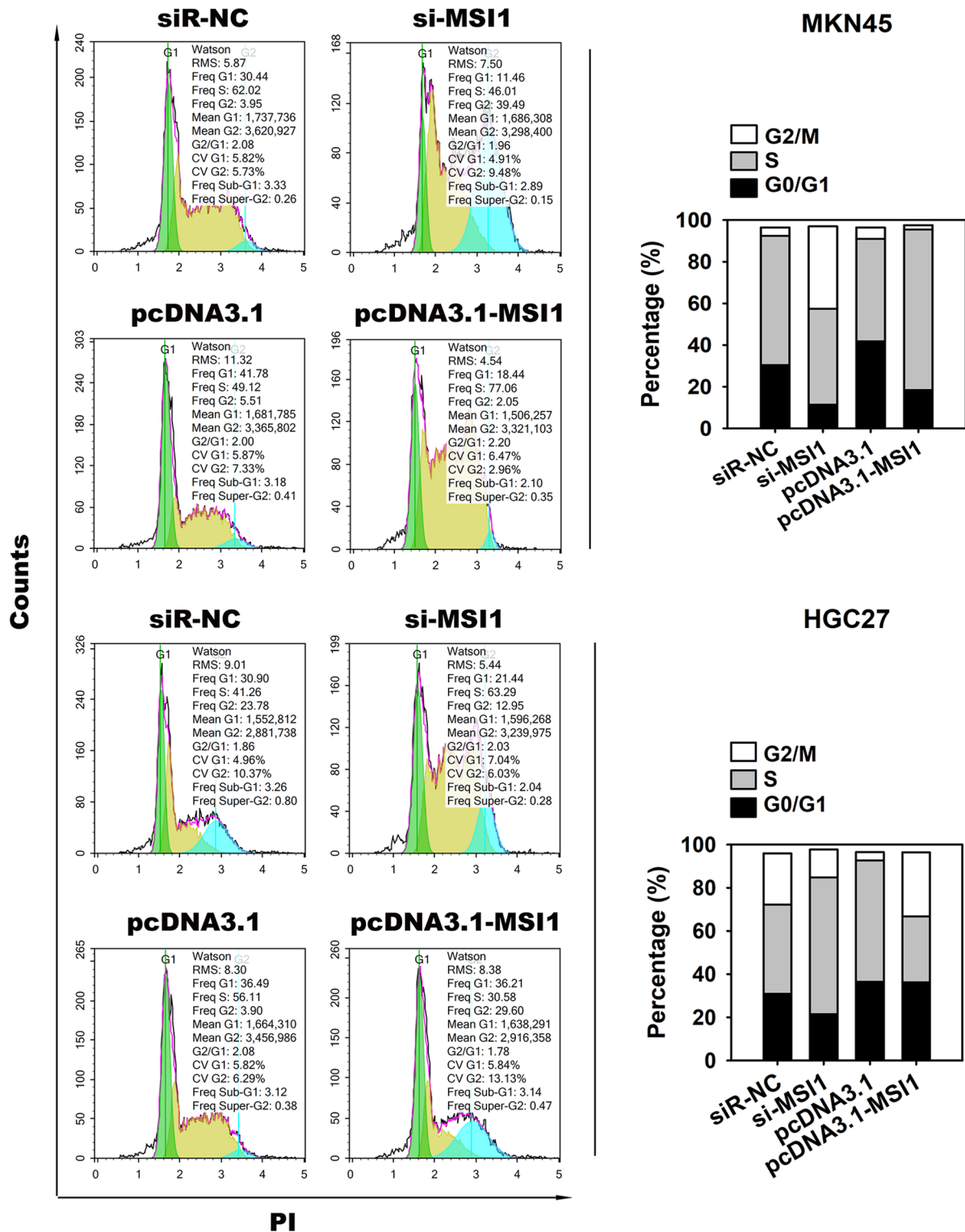


**Figure 4.** Effect of MSI1 interference on the cell cycle. The cell cycle was assessed in MKN45 and HGC27 cells with PI staining and flow cytometry ( $n=3$ ). (A color version of this figure is available in the online journal.)

treatment reduced MSI1 protein levels by 15 days, as shown by Western blotting (Figure 6(a) and (b)). The volumes of tumors were also significantly smaller 15 days after 5-FU and DDP treatment, as well as after MSI1 silencing (Figure 6(c) to (e);  $P < 0.05$  or  $P < 0.01$ ). Tumor sizes differed between the groups that had received combined chemotherapy and MSI1

silencing, compared with the control, after six days (Figure 6(d),  $P < 0.05$  and  $P < 0.01$ , respectively), with marked differences by day 15 (Figure 6(e),  $P < 0.01$ ). Compared with the group treated with both 5-FU and DDP, the tumor volumes in the combined 5-FU and MSI1 knockdown group were significantly reduced (Figure 6(e),  $P < 0.05$ ). We further performed

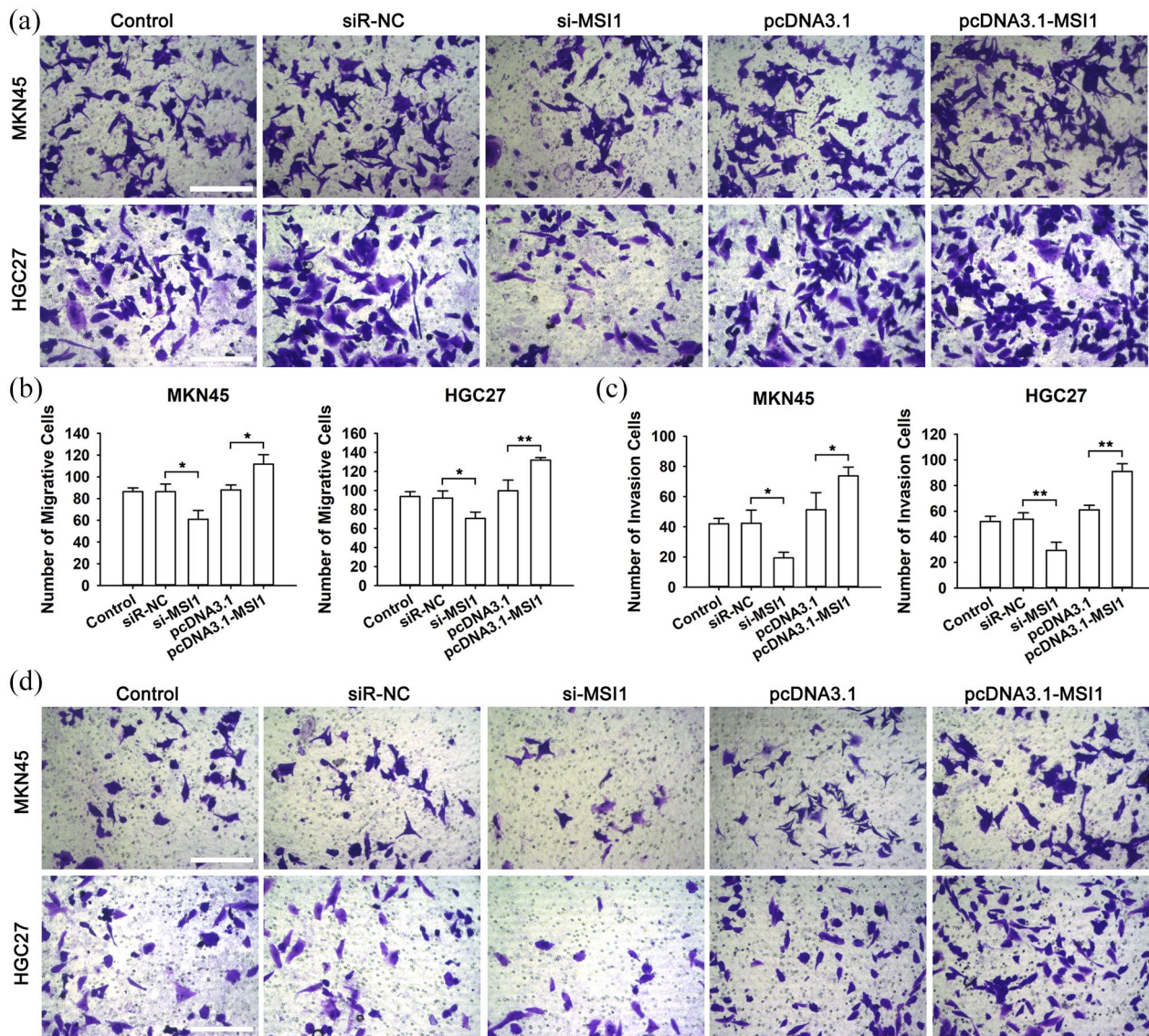


**Figure 5.** Effect of MSI1 on the migration and invasion of MKN45 and HGC27 cells. Images of migrated cells are shown in (a). The quantifications of the migration results are shown in (b). The results suggested that the migration abilities of the cells were significantly inhibited by si-MSI1 and increased by pcDNA3.1-MSI1. The quantifications of the invasion results are shown in (c). Images of invaded cells are shown in (d). The results suggested that the invasion abilities of the cells were significantly inhibited by si-MSI1 and increased by pcDNA3.1-MSI1 (scale bar=200  $\mu$ m.  $n=8-10$  per group; \* $P < 0.05$ ; \*\* $P < 0.01$ ). (A color version of this figure is available in the online journal.)

H&E staining to examine the pathological changes in tumor tissues from the different treatment groups. Compared with control group, the combined 5-FU and MSI1 knockdown group showed reduced tumor cell density in the transplanted PDX model, as shown in Supplementary Figure S1.

### Transcriptome sequencing

The RNA-seq results showed marked differences in gene expression between the silenced MSI1 group and the mock control and MSI1-overexpressing groups. A total of 796 genes showed elevated expression in the silenced group, compared with the controls, with 445 genes that were reduced. Furthermore, in the overexpression group, 799 and 539 were upregulated and downregulated, respectively (Supplementary Figure S2(a)). Gene Ontology (GO) analysis of these genes identified 20 functional categories, with the

most marked changes seen between the silenced and control groups together with the MSI1-overexpressing group (Supplementary Figure S2(b)). The most significant differences were found to be associated with the regulation of apoptosis and angiogenesis. KEGG pathway analysis identified 20 enriched pathways, with the greatest differences seen between the si-MSI1 and control groups and between the si-MSI1 and MSI1-overexpressing groups (Supplementary Table S1, see the Supporting Information). A heatmap also shows the differentially expressed downstream genes (Supplementary Figure S3 and Supplementary Table S2). Most of the pathways modulated by MSI1 appeared to involve translation and signal transduction, implicating the gene in the processing of both genetic and environmental information. BVES was observed to be one of the most upregulated genes, showing an increase of over 2.45-fold (Supplementary Table S2). Western blotting showed that



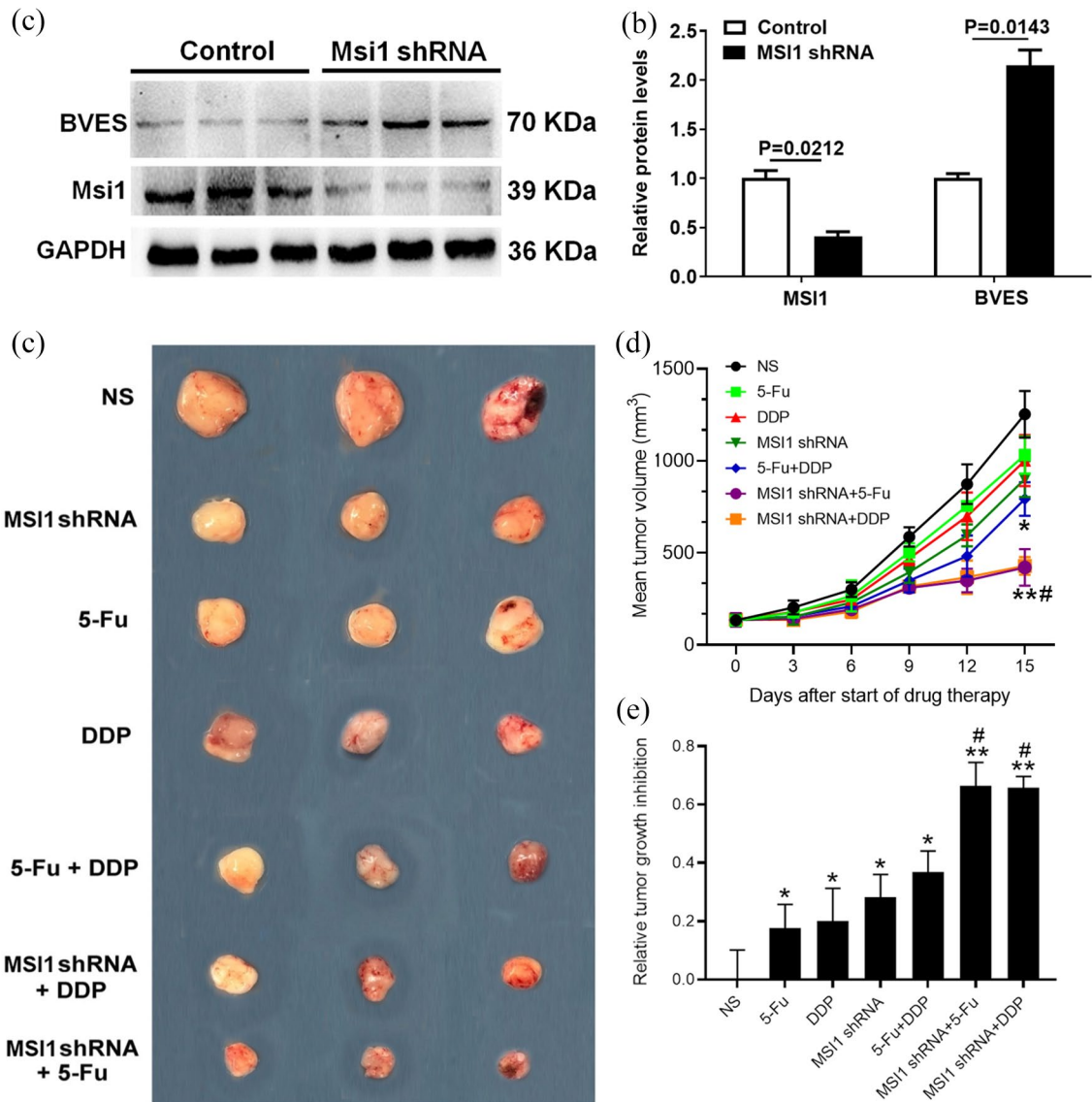


**Figure 6.** MSI1 gene silencing inhibited tumor growth. (a) Representative images of tumors excised after the experiment. (b) The tumor volume curves of the different treatment groups at different time points. (c) The rate of tumor inhibition ( $n=5-6$  animals per group). (d) The Western blot analysis of MSI1 gene silencing in PDX mice. (e) Mean intensity levels of MSI1 and BVES expression ( $*P < 0.05$ ;  $**P < 0.01$  vs the control group (NS);  $#P < 0.05$  vs the 5-Fu and DDP groups). (A color version of this figure is available in the online journal.)

BVES protein levels in the siRNA-MSI1 group showed marked elevation, confirming the RNA-seq findings (Figure 6(a) and (b);  $P=0.0143$ ).

## Discussion

Gastric cancer is currently considered a disease that originates from stem cells.<sup>11</sup> MSI1 is known to be expressed in neural progenitor cells, and has been proposed to be a marker for cancer stem cells, which are known to play vital roles in the development, progression, and expansion of tumors, eventually contributing to chemoresistance and recurrence.<sup>11,14,15</sup> The presence of MSI1 is crucial for maintaining stem cells in an undifferentiated state, and MSI1 has been found to promote proliferation and confer stem cell-like properties on tumor cells.<sup>24,25</sup> Pötschke *et al.*<sup>26</sup> reported that raised MSI1 expression increased chemoresistance in high-grade

pediatric glioma and that MSI1 inhibition improved both the patient outcome and the therapeutic response. Thus, inhibiting MSI1 expression may effectively block the growth, migration, and invasion of cancer cells, suggesting that it could be a reliable target for gastric cancer therapy. However, further investigation is still required to determine the potential of MSI1 as a biomarker for the diagnosis of early gastric cancer or to monitor cancer progression and response to treatment.

Here, in a pilot study of 115 patients screened for gastric cancer, MSI1 was found to be expressed in the patients subsequently diagnosed with gastric cancer. An analysis of archival pathological samples from patients with all stages of gastric cancer showed a relationship between MSI1 and the proliferation markers Ki-67 and PCNA, suggesting a direct relationship between MSI1 and gastric cancer progression. Furthermore, patients with high levels of MSI1 had significantly poorer outcomes than patients with low expression.

We, therefore, undertook to analyze the role of MSI1 in gastric cancer at the mRNA, protein, and cellular levels and to further study its efficacy through designed MSI1-silencing methods *in vivo*. We further constructed specific methods for downregulating and upregulating MSI1 in the MKN45 and HGC27 cell lines. Both transcription and translation of the gene were then verified in the silenced, overexpressing, and control groups by RT-PCR and Western blotting, respectively. We used these systems to evaluate the effects of MSI1 in tumor progression, apoptosis measured by Annexin V/PI staining, the cell cycle analyzed by flow cytometry, proliferation by the MTT assay, and migration using Transwell assays. All these experiments, using both MSI1 silencing and overexpression, showed that MSI1 had a marked influence on the proliferation, migration, and invasion of gastric cancer cells.

To investigate the underlying mechanisms of proliferation inhibition, flow cytometry was used for cell cycle analysis of the MSI1 knockdown and overexpressing cells. During MKN45 cell cycling, chromosome separation and preparation for DNA synthesis take place in the G1 and G2 phases. These processes involve multiple genes which drive the cell cycle.<sup>27</sup> siRNA-MSI1 transfection increased the percentage of MKN45 tumor cells in the G2/M phase, suggesting that MSI1 knockdown might block cell entry into the mitotic phase. Interestingly, the percentage of cells in the G2/M phase was reduced after siRNA-MSI1 transfection in HGC27 cells, and the cells were mostly blocked in the S phase. Although MKN45 and HGC27 cells are both gastric cancer cell lines, they are derived from different sources. Many genes implicated in cell cycle control are omnipresent and are active in a variety of cellular processes, including ubiquitination, transcription, translation, and signal transduction. These genes may influence cancer cell proliferation and apoptosis, as well as the inactivation of tumor suppressor genes and the activation of oncogenes.<sup>27</sup> Thus, further investigation into the roles of cell cycle-associated genes is needed in different gastric cell lines.

Traditional *in vitro* cell tumorigenesis models have generally neglected the molecular characteristics and tumor heterogeneity of the tumor tissue of origin, which may lead to a decrease in the prediction of clinical drug efficacy.<sup>28</sup> The PDX model can compensate for this defect and offers a more accurate prediction of tumor drug efficacy.<sup>28,29</sup> The use of PDX models has proved effective in the study of several cancers, including colorectal, lung, and breast cancer.<sup>30,31</sup> In this study, a PDX mouse model of gastric cancer was established, and was found to maintain the histopathological, genetic, and phenotypic characteristics of the tumor tissues from the original patients. The results showed that si-MSI1 treatment combined with broad-spectrum chemotherapy drugs increased drug sensitivity. Silencing of MSI1 combined with 5-FU or DDP has specific advantages in the treatment of gastric cancer, and its effect was found to be better than that of 5-FU, DDP, or even the combination of these two drugs, indicating that si-MSI1 combination therapy may be superior to the current chemotherapy.

We further analyzed the transcriptomes of the tumor tissue from the PDX models to explore the influence of MSI1 signaling pathways. The transcriptome data from the

MSI1-downregulated samples and MSI1-upregulated samples were compared with those from the control samples to identify abnormally expressed genes. These genes were then investigated and annotated using the GO database, and the relationships between their upstream and downstream signaling pathways were analyzed, indicating that the signaling pathways regulated by MSI1 in gastric cancer include translation and signal transduction pathways. We also found that MSI1 involved in the regulation of the immune and nervous systems, and thus is likely to participate in numerous diseases, including cancer, bacterial and viral infection, and neurodegeneration. Vo *et al.*<sup>32,33</sup> reported that MSI1 regulates multiple processes in medulloblastoma and is required for tumorigenesis. Interestingly, MSI1 expression may be upregulated during the development of the central nervous system (CNS), and downregulated on maturity, suggesting that a lack of MSI1 may be responsible for the inability of the adult CNS to regenerate to any extent.<sup>34</sup> Velasco *et al.*<sup>35</sup> found that MSI1 is a key determinant of cell fate decisions and that abnormal expression of MSI1 contributes to neurodegenerative diseases and glioma development.

It was found that BVES was one of the most dramatically upregulated genes after MSI1 knockdown. This was confirmed by the significant upregulation of BVES protein levels by Western blotting in the siRNA-MSI1-treated mice. BVES is expressed not only in skeletal and cardiac tissue but also in the epithelium throughout the gastrointestinal tract.<sup>36</sup> Its expression is reduced in gastrointestinal cancers, and this reduced expression has been shown in mouse models to promote tumor development.<sup>37,38</sup> The BVES protein is thought to be involved in cell adhesion and movement.<sup>39</sup> Thus, MSI1 may potentially modulate both cell adhesion and movement through suppression of BVES to promote proliferation, suggesting that inhibition of MSI1 may be a therapeutic strategy for cancer treatment. These reports are consistent with our findings, assisting us to further explore the function of MSI1/BVES during translation, signal transduction, and immune regulation for subsequent research. A future direction may be to use coimmunoprecipitation to identify the effects of MSI1, either direct or indirect, in controlling BVES.

## Conclusions

We investigated the relationship between MSI1 expression and the efficacy of chemical drugs in gastric cancer to provide data that might support future clinical trials. Using MSI1 upregulation and downregulation in cell systems, we found that MSI1 modulates proliferation, migration, and invasion, and thus is likely to play a key part in the development and progression of gastric cancer. Experiments using PDX mouse models showed that MSI1 inhibition reduced the tolerance of gastric cancer to chemical drugs. si-MSI1 combined with 5-FU or DDP was effective in reducing tumor sizes and was more effective than the combined use of the two chemical drugs (5-FU and DDP). MSI1 potentially influences the chemotherapeutic effect through BVES pathways. This study provides a strategy for the development of personalized treatment for gastric cancer patients and offers potential value in predicting chemosensitivity in tumors.

**AUTHORS' CONTRIBUTIONS**

F.L., H.Y., X.Z. and Yu.L. performed the experiments and data collection. F.L., X.S., J.Z. and Yi.L. analyzed and interpreted the data. F.L., H.Y., and G.W. wrote and reviewed the manuscript. G.W. and Z.Z. conceived and supervised the entire project. G.W. and Z.Z. revised the manuscript and provided supporting material. All authors read and approved the final manuscript.

**DECLARATION OF CONFLICTING INTERESTS**

The author(s) declared no potential conflicts of interest with respect to the research, authorship, and/or publication of this article.

**ETHICAL APPROVAL**

All procedures involving human participants were performed in accordance with the ethical standards of the Nantong University Affiliated Hospital and with the 1964 Declaration of Helsinki and its later amendments or comparable ethical standards.

**FUNDING**

The author(s) disclosed receipt of the following financial support for the research, authorship, and/or publication of this article: This study was supported by the Natural Science Key Research Program of Jiangsu Province (BE2018778) and the Nantong Science and Technology Project (MSZ18109).

**DATA AVAILABILITY**

All original data are available upon request.

**ORCID ID**

Guohua Wang  <https://orcid.org/0000-0002-4810-8534>

**SUPPLEMENTAL MATERIAL**

Supplemental material for this article is available online.

**REFERENCES**

1. Yin X, Wu Q, Monga J, Xie E, Wang H, Wang S, Zhang H, Wang ZY, Zhou T, Shi Y, Rogers J, Lin H, Min J, Wang F. HDAC1 governs iron homeostasis independent of histone deacetylation in iron-overload Murine models. *Antioxid Redox Signal* 2018;**28**:1224–37
2. Desiderio J, Chao J, Melstrom L, Warner S, Tozzi F, Fong Y, Parisi A, Woo Y. The 30-year experience: a meta-analysis of randomised and high-quality non-randomised studies of hyperthermic intraperitoneal chemotherapy in the treatment of gastric cancer. *Eur J Cancer* 2017;**79**:1–14
3. Digkila A, Wagner AD. Advanced gastric cancer: current treatment landscape and future perspectives. *World J Gastroenterol* 2016;**22**:2403–14
4. Huang S, Guo Y, Li Z, Zhang Y, Zhou T, You W, Pan K, Li W. A systematic review of metabolomic profiling of gastric cancer and esophageal cancer. *Cancer Biol Med* 2020;**17**:181–98
5. Gleeson FC, Kipp BR, Kerr SE, Voss JS, Graham RP, Campion MB, Minot DM, Tu ZJ, Klee EW, Lazaridis KN, Henry MR, Levy MJ. Kinase genotype analysis of gastric gastrointestinal stromal tumor cytology samples using targeted next-generation sequencing. *Clin Gastroenterol Hepatol* 2015;**13**:202–6
6. Kanada M, Kim BD, Hardy JW, Ronald JA, Bachmann MH, Bernard MP, Perez GI, Zarea AA, Ge TJ, Withrow A, Ibrahim SA, Toomajian V, Gambhir SS, Paulmurugan R, Contag CH. Microvesicle-mediated delivery of minicircle DNA results in effective gene-directed enzyme prodrug cancer therapy. *Mol Cancer Ther* 2019;**18**:2331–42
7. Malik YS, Sheikh MA, Xing Z, Guo Z, Zhu X, Tian H, Chen X. Poly-lysine-modified polyethylenimine polymer can generate genetically engineered mesenchymal stem cells for combinational suicidal gene therapy in glioblastoma. *Acta Biomaterialia* 2018;**80**:144–53
8. Okabe M, Sawamoto K, Imai T, Sakakibara S, Yoshikawa S, Okano H. Intrinsic and extrinsic determinants regulating cell fate decision in developing nervous system. *Dev Neurosci* 1997;**19**:9–16
9. Kudinov AE, Karanicolas J, Golemis EA, Boumber Y. Musashi RNA-binding proteins as cancer drivers and novel therapeutic targets. *Clin Cancer Res* 2017;**23**:2143–53
10. Okano H, Kawahara H, Toriya M, Nakao K, Shibata S, Imai T. Function of RNA-binding protein Musashi-1 in stem cells. *Exp Cell Res* 2005;**306**:349–56
11. Kuang RG, Kuang Y, Luo QF, Zhou CJ, Ji R, Wang JW. Expression and significance of Musashi-1 in gastric cancer and precancerous lesions. *World J Gastroenterol* 2013;**19**:6637–44
12. Xiao R, Yu Y, Shen S, Liu F, Kuang R. Musashi1 promotes tumor metastasis and is a prognostic marker for renal carcinoma. *Int J Clin Exp Pathol* 2019;**12**:313–9
13. Guan A, Wang H, Li X, Xie H, Wang R, Zhu Y, Li R. MiR-330-3p inhibits gastric cancer progression through targeting MSI1. *Am J Transl Res* 2016;**8**:4802–11
14. Wang T, Ong CW, Shi J, Srivastava S, Yan B, Cheng CL, Yong WP, Chan SL, Yeoh KG, Iacopetta B, Salto-Tellez M. Sequential expression of putative stem cell markers in gastric carcinogenesis. *Br J Cancer* 2011;**105**:658–65
15. Shou Z, Jin X, He X, Zhao Z, Chen Y, Ye M, Yao J. Overexpression of Musashi-1 protein is associated with progression and poor prognosis of gastric cancer. *Oncol Lett* 2017;**13**:3556–66
16. Lang Y, Kong X, He C, Wang F, Liu B, Zhang S, Ning J, Zhu K, Xu S. Musashi1 promotes non-small cell lung carcinoma malignancy and chemoresistance via activating the Akt signaling pathway. *Cell Physiol Biochem* 2017;**44**:455–66
17. Brungs D, Aghmesheh M, Vine KL, Becker TM, Carolan MG, Ranson M. Gastric cancer stem cells: evidence, potential markers, and clinical implications. *J Gastroenterol* 2016;**51**:313–26
18. Wu H, Li J, Chen J, Yin Y, Da P, Chen Q, Zhang Z, Wang J, Wang G, Qiu X. Efficacy of radiation exposure in laryngeal squamous cell carcinoma is mediated by the LAMP3/LAMC2/tenascin-C pathway. *Exp Biol Med* 2019;**244**:1070–80
19. Gao H, Korn JM, Ferretti S, Monahan JE, Wang Y, Singh M, Zhang C, Schnell C, Yang G, Zhang Y, Balbin OA, Barbe S, Cai H, Casey F, Chatterjee S, Chiang DY, Chuai S, Cogan SM, Collins SD, Dammassa E, Ebel N, Embry M, Green J, Kauffmann A, Kowal C, Leary RJ, Lehar J, Liang Y, Loo A, Lorenzana E, Robert McDonald E 3rd, McLaughlin ME, Merkin J, Meyer R, Naylor TL, Patawaran M, Reddy A, Röelli C, Ruddy DA, Salangsang F, Santacrose F, Singh AP, Tang Y, Tinetto W, Tobler S, Velazquez R, Venkatesan K, Von Arx F, Wang HQ, Wang Z, Wiesmann M, Wyss D, Xu F, Bitter H, Atadja P, Lees E, Hofmann F, Li E, Keen N, Cozens R, Jensen MR, Pryer NK, Williams JA, Sellers WR. High-throughput screening using patient-derived tumor xenografts to predict clinical trial drug response. *Nat Med* 2015;**21**:1318–25
20. Gao C, Yuan X, Jiang Z, Gan D, Ding L, Sun Y, Zhou J, Xu L, Liu Y, Wang G. Regulation of AKT phosphorylation by GSK3 $\beta$  and PTEN to control chemoresistance in breast cancer. *Breast Cancer Res Treat* 2019;**176**:291–301
21. Lin S, Wang H, Yang W, Wang A, Geng C. Silencing of long non-coding RNA colon cancer-associated transcript 2 inhibits the growth and metastasis of gastric cancer through blocking mTOR signaling. *Onco Targets Ther* 2020;**13**:337–49
22. Sakurai Y, Uruguchi T, Imazu H, Hasegawa S, Matsubara T, Ochiai M, Funabiki T. Changes in thymidylate synthase and its inhibition rate and changes in dihydropyrimidine dehydrogenase after the administration of 5-fluorouracil with cisplatin to nude mice with gastric cancer xenograft SC-1-NU. *Gastric Cancer* 2004;**7**:110–6
23. Guo XF, Liu JP, Ma SQ, Zhang P, Sun WD. Avicularin reversed multidrug-resistance in human gastric cancer through enhancing Bax and BOK expressions. *Biomed Pharmacother* 2018;**103**:67–74

24. Ito T, Kwon HY, Zimdahl B, Congdon KL, Blum J, Lento WE, Zhao C, Lagoo A, Gerrard G, Foroni L, Goldman J, Goh H, Kim SH, Kim DW, Chuah C, Oehler VG, Radich JP, Jordan CT, Reya T. Regulation of myeloid leukaemia by the cell-fate determinant Musashi. *Nature* 2010;**466**:765–8
25. Bobryshev YV, Freeman AK, Botelho NK, Tran D, Levert-Mignon AJ, Lord RV. Expression of the putative stem cell marker Musashi-1 in Barrett's esophagus and esophageal adenocarcinoma. *Dis Esophagus* 2010;**23**:580–9
26. Pötschke R, Gielen G, Pietsch T, Kramm C, Klusmann JH, Hüttelmaier S, Kühnöl CD. Musashi1 enhances chemotherapy resistance of pediatric glioblastoma cells in vitro. *Pediatr Res* 2020;**87**:669–76
27. Chen L, Lan B, Chen XH, Li JF, Qu Y, Yu BQ, Yu YY, Gu QL, Zhu ZG, Liu BY. Cell cycle dependent genes from the gastric cancer cell MKN45 can affect tumorigenesis. *Hepatogastroenterology* 2011;**58**:674–81
28. Jung J, Seol HS, Chang S. The generation and application of patient-derived xenograft model for cancer research. *Cancer Res Treat* 2018;**50**:1–10
29. Weeber F, Ooft SN, Dijkstra KK, Voest EE. Tumor organoids as a pre-clinical cancer model for drug discovery. *Cell Chem Biol* 2017;**24**:1092–100
30. Siolas D, Hannon GJ. Patient-derived tumor xenografts: transforming clinical samples into mouse models. *Cancer Res* 2013;**73**:5315–9
31. Inoue T, Terada N, Kobayashi T, Ogawa O. Patient-derived xenografts as in vivo models for research in urological malignancies. *Nat Rev Urol* 2017;**14**:267–83
32. Vo DT, Subramaniam D, Remke M, Burton TL, Uren PJ, Gelfond JA, de Sousa Abreu R, Burns SC, Qiao M, Suresh U, Korshunov A, Dubuc AM, Northcott PA, Smith AD, Pfister SM, Taylor MD, Janga SC, Anant S, Vogel C, Penalva LO. The RNA-binding protein Musashi1 affects medulloblastoma growth via a network of cancer-related genes and is an indicator of poor prognosis. *Am J Pathol* 2012;**181**:1762–72
33. Bish R, Vogel C. RNA binding protein-mediated post-transcriptional gene regulation in medulloblastoma. *Mol Cells* 2014;**37**:357–64
34. Glazer RI, Vo DT, Penalva LOF. Musashi1: an RBP with versatile functions in normal and cancer stem cells. *Front Biosci-Landmark* 2012;**17**:54–64
35. Velasco MX, Kosti A, Guardia GDA, Santos MC, Tegge A, Qiao M, Correa BRS, Hernandez G, Kokovay E, Galante PAF, Penalva LOF. Antagonism between the RNA-binding protein Musashi1 and miR-137 and its potential impact on neurogenesis and glioblastoma development. *RNA* 2019;**25**:768–82
36. Parang B, Thompson JJ, Williams CS. Blood Vessel Epicardial Substance (BVES) in junctional signaling and cancer. *Tissue Barr* 2018;**6**:1–12
37. Page KA, Seo D, Belfort-DeAguiar R, Lacadie C, Dzuira J, Naik S, Amarnath S, Constable RT, Sherwin RS, Sinha R. Circulating glucose levels modulate neural control of desire for high-calorie foods in humans. *J Clin Invest* 2011;**121**:4161–9
38. Kim M, Jang HR, Haam K, Kang TW, Kim JH, Kim SY, Noh SM, Song KS, Cho JS, Jeong HY, Kim JC, Yoo HS, Kim YS. Frequent silencing of popeye domain-containing genes, BVES and POPDC3, is associated with promoter hypermethylation in gastric cancer. *Carcinogenesis* 2010;**31**:1685–93
39. Hager HA, Bader DM. Bves: ten years after. *Histol Histopathol* 2009;**24**:777–87

(Received October 26, 2021, Accepted January 11, 2022)